



Electromagnetic Fault Analysis of a Power Transformer Using Ansys@ Maxwell

Ismail Sarıgül ^{1*} , Müslüm Arkan ¹ 
M. Salih Mamiş ¹ , Taner Goktas ² 

¹ Inonu University, Malatya, Türkiye

²Dokuz Eylul University, İzmir, Türkiye

ismail.sarigul@inonu.edu.tr

Abstract. Power transformers are among the most critical components in electrical energy systems, serving to convert voltage levels and ensure the reliable transmission of power. Therefore, modeling and analyzing possible transformer faults in advance is essential for maintaining system continuity and operational safety. In this study, a three-dimensional model of a laboratory-based power transformer was developed using ANSYS@ Maxwell. Manufacturer data were utilized during the modeling process, and electromagnetic analyses were conducted considering the core geometry, winding configuration, material properties, and associated losses. The model accuracy was verified by comparing the simulated turns ratio, no-load losses, and load losses with the factory test results. Subsequently, phase-to-phase and phase-to-ground short-circuit faults were simulated on the model. The variations in current, voltage, and electromagnetic force before and after the faults were analyzed in detail. The results reveal the impacts of fault conditions on magnetic saturation, winding stress, and voltage imbalance within the transformer. Overall, the findings provide valuable insight into the short-circuit behavior of power transformers and serve as a useful reference for the early detection of faults and the improvement of protection systems in power networks.

Keywords: Power Transformer, Ansys@Maxwell, Fault Analysis.

1 Introduction

Transformers are among the most critical components involved in the transmission and distribution of electrical energy. Therefore, faults occurring in these components may lead to severe consequences. Since the continuity of energy supply is of great importance today, the detection of faults that arise in transformers has become equally significant. Approximately 30% of transformer failures originate from winding-related faults [1]. Faults occurring in transformer windings constitute a major threat to the uninterrupted and reliable delivery of electrical power to consumers. Such faults typically begin with the weakening of winding insulation as a result of lightning impulses, partial discharges, or switching operations. The degradation of insulation leads to arc formation between windings and the emergence of high-amplitude short-circuit currents due to conductor-to-conductor contact. This situation causes severe mechani-

cal and thermal stresses on the windings, which may ultimately result in permanent damage. If the fault is not detected and eliminated at an early stage, the transformer may be completely taken out of service, making prolonged power outages inevitable [2].

A winding-to-ground fault occurs when weakened insulation allows the winding to come into direct contact with ground potential. In such faults, the sudden reduction of internal winding resistance and winding-to-ground impedance generates high-amplitude short-circuit currents and pronounced dielectric stresses [3]. A winding-to-winding (phase-to-phase) fault involves a direct conductive contact resulting from insulation breakdown between two phase windings. In this condition, the magnetic flux distribution becomes distorted, short-circuit currents rise sharply and abruptly, and intense mechanical forces develop on the windings—leading to irreversible damage unless immediate intervention is applied [4,5].

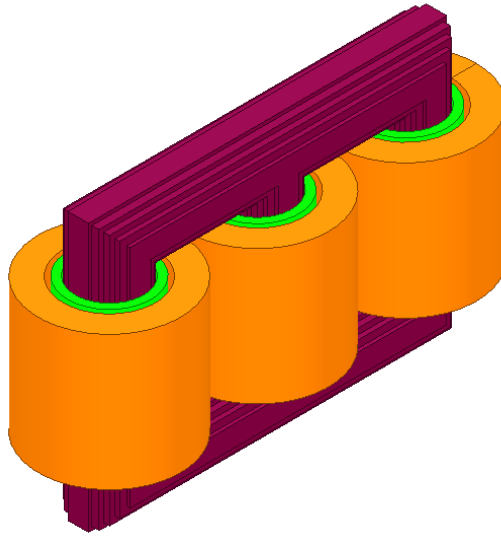
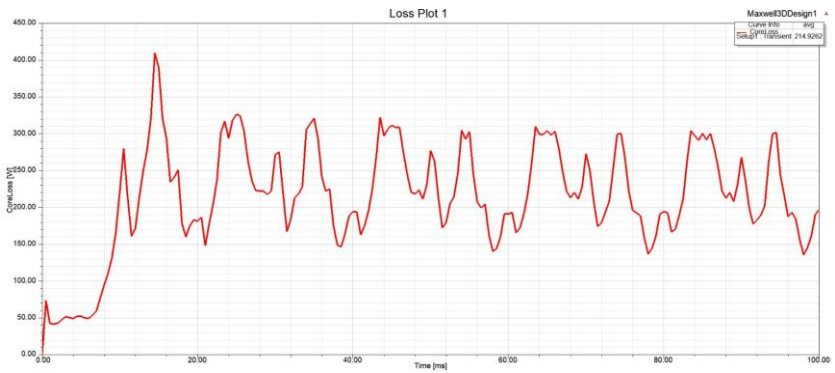
Electromagnetic analyses performed in ANSYS@Maxwell provide highly accurate results for transformer design and fault modeling. In multiphase transformer structures, the finite element analysis (FEA) technique enables the optimization of magnetic flux distribution, winding impedances, and losses. For example, in the study conducted by Hacan, Kabas, and Ogüten [6], a three-phase transformer was designed using ANSYS@Maxwell to minimize volume and losses. Similarly, Alpsalaz and Mamiş [7] investigated the time-dependent behavior of high-frequency harmonics and electromagnetic forces under inter-winding arc and short-circuit conditions using a MATLAB@ANSYS Maxwell co-simulation environment. In addition, Özüpak [8] examined magnetic flux density, short-circuit current, and winding-core mechanical strength under various loading conditions in distribution transformers, identifying critical stress regions during fault events. These studies demonstrate that ANSYS @Maxwell is an effective tool for detailed modeling of transformers under both normal operating conditions and fault scenarios.

2 Method and Modelling

In this section, a three-phase transformer was modeled in Ansys@Maxwell using the data provided by the manufacturer. The accuracy of the designed model was verified by comparing the simulation results with the manufacturer's specifications. Key factory parameters—such as guaranteed no-load losses and voltage ratio—were evaluated against the model outputs, confirming the validity and reliability of the developed transformer model. The data provided by the manufacturer are presented in Table 1. In the first stage, the simulation was carried out under fault-free operating conditions. In this case, the current, voltage, and force waveforms corresponding to normal operating conditions were obtained.

Table 1. Transformer Data

Factory Info	Data
HV/LV Voltages	10,000/400 V
HV/LV connection Type	YNyn0
Number of Phases	3
Core Losses	220 W
Number of HV/LV Turns	1750/70

**Fig. 1.** Ansys@Maxwell Transformer Model**Fig. 2.** Transformer Core Loss

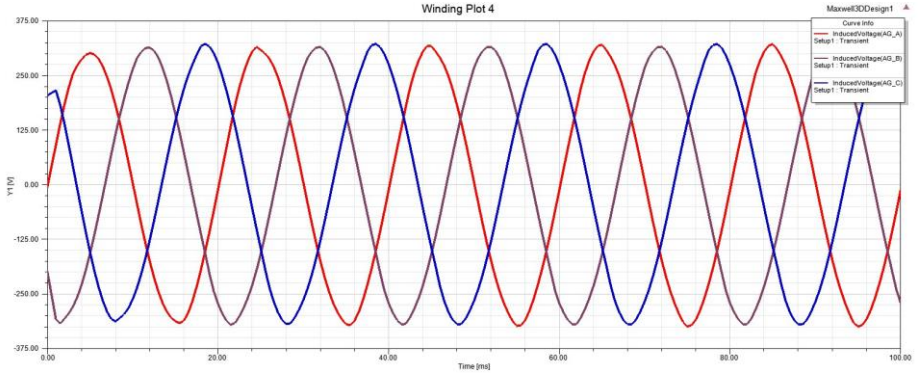


Fig. 3. Low Voltage Side Voltages

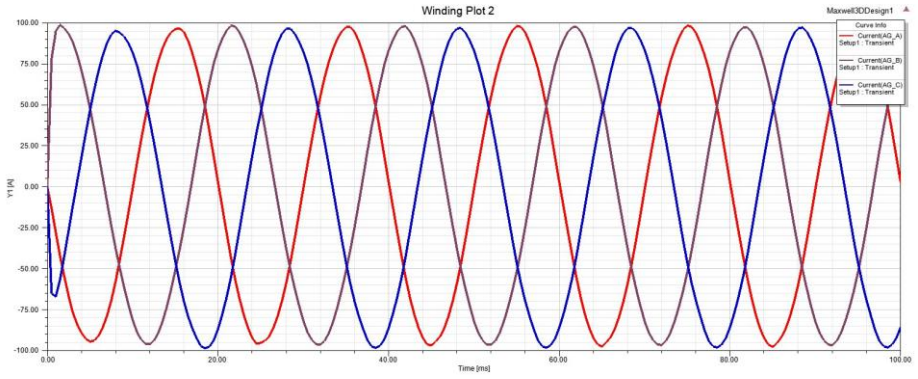


Fig. 4. Low Voltage Side Currents

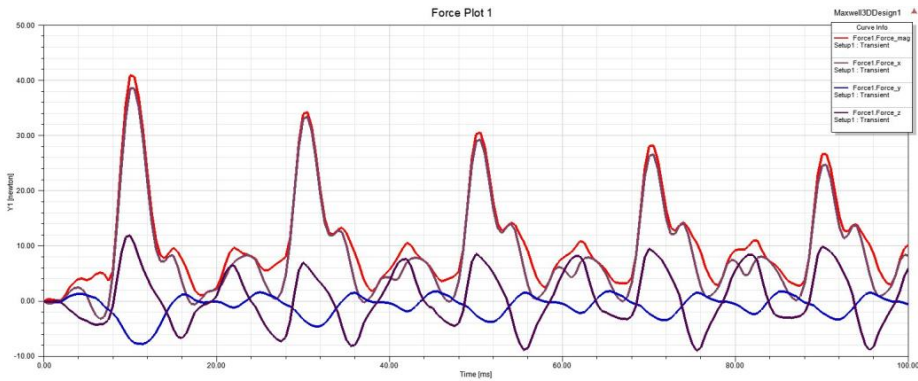


Fig. 5. Electromagnetic force on the windings

3 Fault Analysis

Winding-to-winding faults in transformers typically originate from the weakening of turn-to-turn or layer-to-layer insulation and rapidly progress into localized short-circuit regions due to high-voltage impulses, switching transients, or the mechanical forces induced by short-circuit currents. These faults lead to rapid rises in current—often challenging the thresholds of differential protection systems—and cause abrupt changes in winding impedance [9]. Winding-to-ground faults, on the other hand, usually occur when the dielectric strength of the oil–paper insulation between the winding and the core deteriorates due to moisture ingress, aging, or contamination, often preceded by partial discharge activity [10]. According to CIGRÉ failure statistics, winding-to-winding and winding-to-ground faults rank among the most critical failure modes in large power transformers, constituting a substantial portion of total transformer faults [11]. Thermal degradation of insulation, along with moisture and decomposition by-products in the oil, significantly accelerates the progression of these fault types, leading to early dielectric breakdown [12].

In the simulation process, the transformer model created in the Ansys@ Maxwell was transferred to the Twin Builder circuit platform. The fault scenarios were then implemented and analyzed within the Twin Builder simulation environment.

3.1 Winding-to-Ground Fault

The simulation was executed for 0.1 s. At 0.05 s, phase A of the low-voltage side was connected to ground, creating a phase-to-ground fault. Following the fault initiation, the low-voltage side exhibited the waveforms presented below.

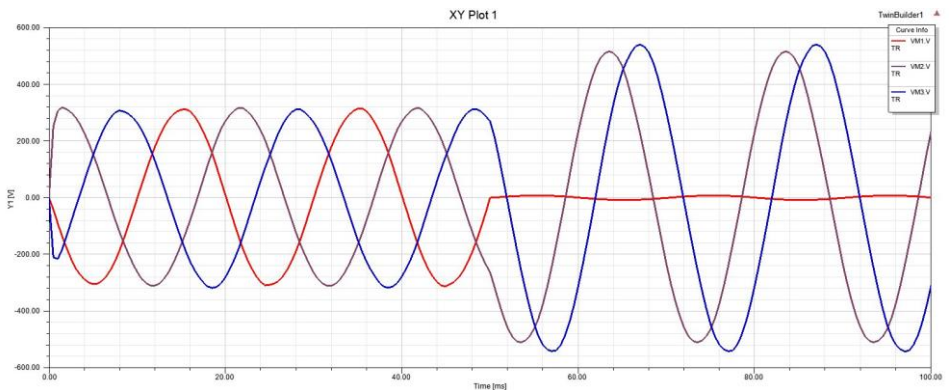


Fig. 6. Low-Voltage Side Phase Voltage in Phase-Ground Fault

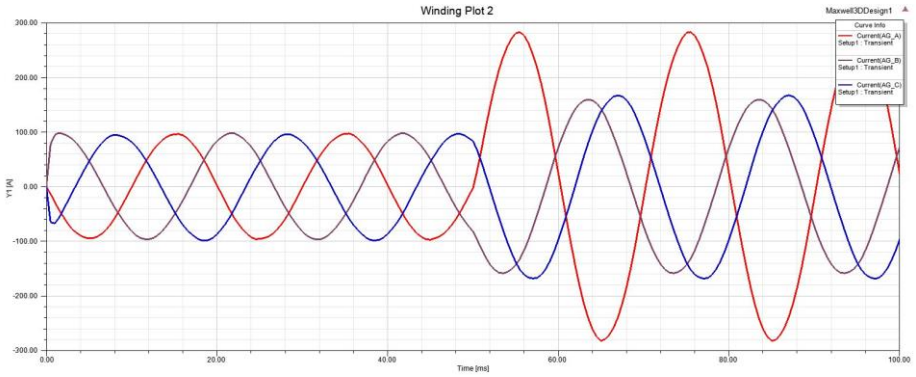


Fig. 7. Low-Voltage Side Phase Currents in Phase-Ground Fault

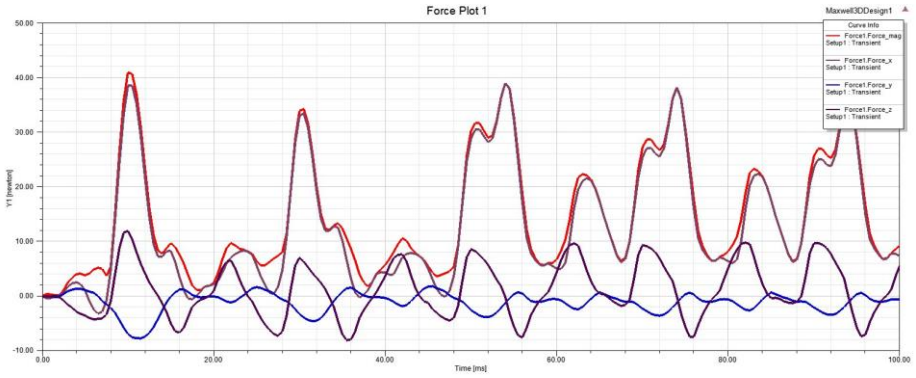


Fig. 8. Electromagnetic Force on the Windings in Phase-Ground Fault

3.2 Winding-to-Winding Fault

In the winding-to-winding fault model, the A and B windings were short-circuited at 0.05 s. Following the initiation of the fault, the low-voltage side produced the wave-forms presented below.

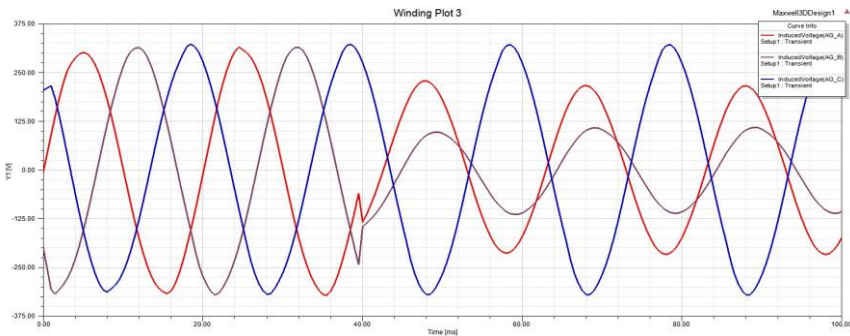


Fig. 9. Low-Voltage Side Phase Voltage in Phase-Phase Fault



Fig. 10. Low-Voltage Side Phase Current in Phase-Phase Fault

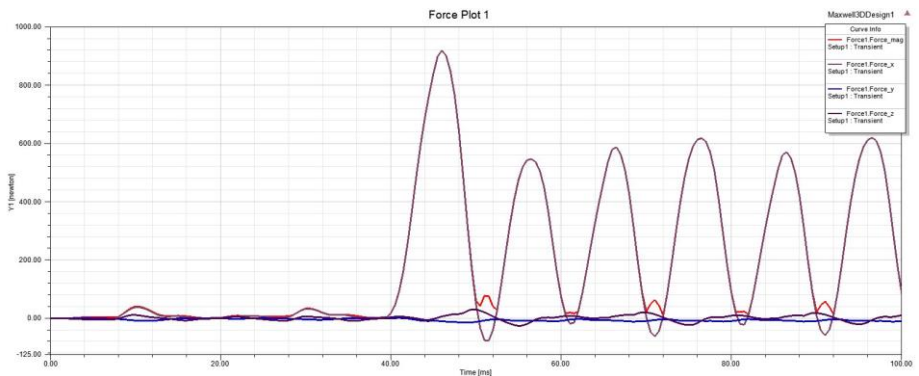


Fig. 11. Electromagnetic Force on the Windings in Phase-Phase Fault

The faults were applied at $t = 0.05$ s, allowing a clear comparison between the pre-fault steady-state condition and the post-fault transient response.

In the winding-to-ground fault scenario, the current waveforms exhibited an instantaneous and pronounced rise in the faulted phase. The current in the affected phase increased to several times its nominal value, while distortions appeared in the other phases due to magnetic coupling and asymmetric flux distribution. The voltage waveforms collapsed in the faulted phase, producing nearly zero or severely suppressed voltage levels. Mechanical force analysis confirmed this behavior: following the fault, large and repetitive electromagnetic force peaks emerged in the corresponding phase, resulting in significant radial and axial stresses on the windings. Such behavior is characteristic of a low-impedance ground short-circuit.

In contrast, the winding-to-winding (interturn) short circuit produced an entirely different transient response. Since only a few turns were shorted, the terminal currents initially remained close to their nominal sinusoidal form, with only minor distortions. However, the induced voltage waveforms exhibited an abrupt drop and sharp distortion at the instant the fault was applied, indicating localized disruption in flux linkage within the winding. More importantly, mechanical forces increased dramatically after the fault and reached levels significantly higher than those observed in the winding-

to-ground fault. This is attributed to the very large localized circulating currents generated within the shorted loop. Consequently, although an interturn fault may present limited external electrical symptoms, it causes much more severe internal electromechanical stresses and becomes considerably more difficult to detect with conventional protection schemes.

4 Conclusion

In this study, a three-phase distribution transformer was modeled in the Ansys@Maxwell and dynamically co-simulated with Twin Builder to examine the transient behavior of two fundamental internal fault scenarios: winding-to-ground (phase-to-ground) and winding-to-winding (interturn) short-circuit faults. The faults were applied at $t = 0.05$ s, allowing a clear comparison between the pre-fault steady-state condition and the post-fault transient response.

In the winding-to-ground fault scenario, the current waveforms exhibited an instantaneous and pronounced rise in the faulted phase. The current in the affected phase increased to several times its nominal value, while distortions appeared in the other phases due to magnetic coupling and asymmetric flux distribution. The voltage waveforms collapsed in the faulted phase, producing nearly zero or severely suppressed voltage levels. Mechanical force analysis confirmed this behavior: following the fault, large and repetitive electromagnetic force peaks emerged in the corresponding phase, resulting in significant radial and axial stresses on the windings. Such behavior is characteristic of a low-impedance ground short-circuit.

In contrast, the winding-to-winding (interturn) short circuit produced an entirely different transient response. Since only a few turns were shorted, the terminal currents initially remained close to their nominal sinusoidal form, with only minor distortions. However, the induced voltage waveforms exhibited an abrupt drop and sharp distortion at the instant the fault was applied, indicating localized disruption in flux linkage within the winding. More importantly, mechanical forces increased dramatically after the fault and reached levels significantly higher than those observed in the winding-to-ground fault. This is attributed to the very large localized circulating currents generated within the shorted loop. Consequently, although an interturn fault may present limited external electrical symptoms, it causes much more severe internal electromechanical stresses and becomes considerably more difficult to detect with conventional protection schemes.

A comparison of the two fault types leads to the following conclusions:

- A winding-to-ground fault produces high terminal currents, voltage collapse, and moderate levels of mechanical stress.
- An interturn fault exhibits limited external electrical indications, yet generates extremely high internal electromagnetic forces and poses a greater risk of winding deformation.
- Under healthy operating conditions, all current, voltage, and force components are balanced and sinusoidal. Both fault types disrupt this balance; however, each produces a distinct electrical–mechanical signature.

In conclusion, the Maxwell–Twin Builder co-simulation successfully captured the multiphysics nature of transformer faults. The findings indicate that, although inter-turn faults exhibit weak electrical signatures, their mechanical effects are severe, necessitating advanced detection techniques such as flux-based indicators and force/vibration monitoring. In contrast, winding-to-ground faults produce more pronounced current and voltage deviations, allowing them to be detected more easily using conventional protection methods. This study demonstrates that the reliable diagnosis of internal transformer faults requires the combined assessment of both electromagnetic and mechanical analyses.

Acknowledgments

This study was supported by the Scientific and Technological Research Council of Turkey (TUBITAK) under the Grant Number 123E658. The authors thank to TUBITAK for their supports.

References

1. Metwally, I.A.: Failures, monitoring and new trends of power transformers. *IEEE Potentials* **30**(3), 36–43 (2011). <https://doi.org/10.1109/MPOT.2011.940233>
2. Akdağ, M., Keleş, C., Mamiş, M.: A novel method for detection of power transformer internal arcs using alternative transient program–electromagnetic transients program (2024)
3. Chiradeja, P., Ngaopitakkul, A.: Winding-to-ground fault location in power transformer windings using combination of discrete wavelet transform and back-propagation neural network. *Scientific Reports* **12**, 20157 (2022). <https://doi.org/10.1038/s41598-022-24434-9>
4. Abbasi, M.: Diagnosis of inter-turn faults in power transformers using electromagnetic field analysis and vibration response. *Electric Power Systems Research* **212**, 108601 (2022)
5. Beheshti Asl, N., Yazdani-Asrami, M., Huang, H.: Investigation of winding deformation and short-circuit mechanical stresses in distribution transformers using coupled field analysis. *International Journal of Electrical Power & Energy Systems* **169**, 109116 (2025)
6. Hacan, M., Kabas, B., Oğüten, M.: Design optimization of a three-phase power transformer using ANSYS Maxwell finite-element analysis. arXiv:2201.11769 (2022)
7. Alpsalaz, A., Mamiş, H.: Transient analysis of inter-winding arc faults in transformers using coupled Matlab–ANSYS Maxwell approach. *Applied Sciences* **14**(20), 9335–9348 (2024)
8. Özüpak, M.: Magnetic flux and short-circuit current analysis of distribution transformers under varying load conditions using ANSYS Maxwell. *Journal of Research and Communication in Engineering* **18**(3), 45–52 (2021)
9. IEEE Std C57.12.90-2015: IEEE Standard Test Code for Liquid-Immersed Distribution, Power, and Regulating Transformers (2015)

10. Saha, T.K.: Review of modern diagnostic techniques for assessing insulation condition in aged transformers. *IEEE Transactions on Dielectrics and Electrical Insulation* **10**(5), 903–917 (2003)
11. CIGRÉ WG A2.37: Transformer Reliability Survey (2015)
12. Tenbohlen, S., Kachler, D.J.: Condition assessment of power transformers using oil analysis and dissolved gas analysis. *IEEE Electrical Insulation Magazine* **19**(2), 22–30 (2002)

Open Access This chapter is licensed under the terms of the Creative Commons Attribution-NonCommercial 4.0 International License (<http://creativecommons.org/licenses/by-nc/4.0/>), which permits any noncommercial use, sharing, adaptation, distribution and reproduction in any medium or format, as long as you give appropriate credit to the original author(s) and the source, provide a link to the Creative Commons license and indicate if changes were made.

The images or other third party material in this chapter are included in the chapter's Creative Commons license, unless indicated otherwise in a credit line to the material. If material is not included in the chapter's Creative Commons license and your intended use is not permitted by statutory regulation or exceeds the permitted use, you will need to obtain permission directly from the copyright holder.

